Hyperfine structure of the $1\,^3\Delta_g$, $2\,^3\Pi_g$, and $3\,^3\Sigma_g^+$ states of $^6Li^7Li$

Li Li[a)]
Department of Physics and Key Lab of Atomic and Molecular Nanosciences, Tsinghua University, Beijing 100084, China

Angelos Lazoudis
Physics Department, Temple University, Philadelphia, Pennsylvania 19122

Peng Yi and Yaoming Liu
Department of Physics and Key Lab of Atomic and Molecular Nanosciences, Tsinghua University, Beijing 100084, China

John Huennekens
Department of Physics, Lehigh University, Bethlehem, Pennsylvania 18015

Robert W. Field
Department of Chemistry, Massachusetts Institute of Technology, Cambridge, Massachusetts 02139

A. Marjatta Lyyra
Physics Department, Temple University, Philadelphia, Pennsylvania 19122

(Received 29 January 2002; accepted 26 March 2002)

The hyperfine splittings of the $1\,^3\Delta_g$, $2\,^3\Pi_g$, and $3\,^3\Sigma_g^+$ states of $^6Li^7Li$ have been resolved by sub-Doppler, continuous wave, perturbation facilitated optical–optical double resonance excitation spectroscopy through newly identified $A\,^1\Sigma_u^+$ $(v_A'=5, J'=24)\sim b\,^3\Pi_u$ $(v_b'=12, N'=23, J'=24)$ mixed *window* levels. The $3\,^3\Sigma_g^+$ and $1\,^3\Delta_g$ states follow the case $b_{\beta S}$ coupling scheme. The Fermi contact interaction between the ^7Li nucleus and the electron spin is the dominant term for the observed hyperfine splittings. The Fermi contact constants for the ^7Li nucleus in the $^6Li^7Li$ molecule have been determined to be 110 MHz for the $3\,^3\Sigma_g^+$ state and 107 MHz for the $1\,^3\Delta_g$ state. The $2\,^3\Pi_g$ state has doubly excited character and its hyperfine coupling is different from that of the $3\,^3\Sigma_g^+$ and $1\,^3\Delta_g$ states. The Fermi contact constants of triplet Rydberg states of $^6Li^7Li$ versus $^7Li_2$ are discussed, and insights into the physical basis for case $b_{\beta S}$ coupling are illustrated. © *2002 American Institute of Physics.* [DOI: 10.1063/1.1478692]

I. INTRODUCTION

Molecular hyperfine structure (HFS) comes from the interaction of the magnetic dipole moment and/or electric quadrupole moment of the nuclei with other angular momenta (electron spin, electronic orbital angular momentum, nuclear rotation, etc.). When the molecule has a $\sigma(ns)$ valence orbital and a nonzero electronic spin, the Fermi contact interaction, $b\mathbf{I}\cdot\mathbf{S}$, is usually the dominant hyperfine interaction term. Thus the hyperfine splitting can provide direct information about the electron spin density at the nucleus. In other words, the hyperfine splitting gives direct evidence about the electronic configuration, which cannot be obtained from the vibration-rotation structure alone.

The nuclear spins of the Na and ^7Li atoms are both 3/2. The hyperfine splittings of several triplet Rydberg states of Na_2 and $^7Li_2$ have been resolved by sub-Doppler, perturbation facilitated optical–optical double resonance (PFOODR) excitation spectroscopy.[1–9] All previously observed triplet Rydberg states of Na_2 and $^7Li_2$ (with the exception of the Na_2 $2\,^3\Pi_g$ and $3\,^3\Pi_g$ states and low-N levels of the Na_2 $1\,^3\Delta_g$ state) follow the case $b_{\beta S}$ coupling scheme. In this coupling scheme, the total nuclear spin angular momentum, **I**, first couples to the total electron spin angular momentum, **S**, to yield **G** (**G**=**I**+**S**), and then **G** couples to **N** to yield the total angular momentum **F** (**F**=**N**+**G**). Each rotational level, N, splits into $2I+1$ or $2S+1$ (whichever is smaller) G components, described by

$$E_{G,I,S}=(b/2)[G(G+1)-I(I+1)-S(S+1)], \qquad (1)$$

where b is the Fermi contact constant, which is independent of N and arises almost entirely from the singly occupied σ_g valence orbital common to all $[\sigma_g(ns)]^1[(ml)\lambda_{g/u}]^1$ triplet Rydberg states. The G components have been resolved in sub-Doppler, CW, PFOODR excitation spectra of Na_2 and $^7Li_2$. The predicted values for the Fermi contact interaction constants, b, for all Na_2 and $^7Li_2$ Rydberg states are $\sim\frac{1}{4}$ the value of the Fermi contact constant of the corresponding atomic ^2S ground state (for $^7Li\,2s\,^2S$ $b=402$ MHz, for $Na\,3s\,^2S$ $b=886$ MHz).[1] This is based on the idea that these Rydberg states are built on the M_2^+ $X\,^2\Sigma_g^+$ ion-core ground state. The experimentally determined values of the Fermi contact constants of Na_2 and $^7Li_2$ are ~210–220 MHz and ~100 MHz, respectively, which are in very good agreement with the predicted values.

The nuclear spin of the ^6Li atom is 1 and the Fermi contact constant of the $2s\,^2S$ atomic state is 152 MHz.

[a)]Author to whom correspondence should be addressed.

 © 2002 American Institute of Physics

Downloaded 25 Aug 2002 to 128.180.23.36. Redistribution subject to AIP license or copyright, see http://ojps.aip.org/jcpo/jcpcr.jsp

Therefore it is very interesting to compare the hyperfine splittings of the triplet states of $^6Li^7Li$ with those of the triplet states of $^7Li_2$.

Recently, a new pair of $A\,^1\Sigma_u^+ \sim b\,^3\Pi_u$ mixed levels of $^6Li^7Li$, $A\,^1\Sigma_u^+$ $(v'_A=5, J'=24) \sim b\,^3\Pi_u$ $(v'_b=12, N'=23, J'=24)$, was identified.[10] These two mixed levels have been used as intermediate *window* levels in the study of the triplet Rydberg states of $^6Li^7Li$ by both CW and pulsed PFOODR excitation spectroscopy.[10,11] Vibronic levels of the $2\,^3\Delta_g$ state have been observed via these new *window* levels by pulsed PFOODR excitation,[10] and vibronic levels of the $1\,^3\Delta_g$, $2\,^3\Pi_g$, and $3\,^3\Sigma_g^+$ states of $^6Li^7Li$ have been observed by CW PFOODR excitation.[11] Hyperfine structure has been resolved in the CW PFOODR excitation spectra. Here we report the hyperfine structure of the $1\,^3\Delta_g$, $2\,^3\Pi_g$, and $3\,^3\Sigma_g^+$ states.

II. EXPERIMENT

The experimental setup is the same as in our previous PFOODR fluorescence excitation study of $^7Li_2$.[5,6] Briefly, natural isotopic abundance lithium metal was heated in a five-arm heatpipe oven. Argon gas was used as the buffer gas at a pressure of 0.3–0.5 Torr, which corresponds to an oven temperature of about 1000 K in the active region of the heatpipe. In the vapor the percentage of Li_2 molecules at 1000 K is about 2.8%,[12] with the composition being 85.7% $^7Li_2$, 0.55% $^6Li_2$, and 13.74% $^6Li^7Li$. Two single-mode, frequency stabilized CW dye lasers (1 MHz linewidth) were used as the *pump* and *probe* lasers in a counter-propagating geometry along the axis of the heatpipe. The *pump* laser was operated with DCM dye and its output was 300–600 mW; the *probe* laser was operated with DCM dye (200–400 mW) or R6G dye (400–600 mW). The *pump* laser excited the $A\,^1\Sigma_u^+$ $(v'_A=5, J'=24) \sim b\,^3\Pi_u$ $(v'_b=12, N'=23, J'=24)$ $\leftarrow X\,^1\Sigma_g^+$ $(v''=0, J''=23$ or $25)$ transition and the *probe* laser frequency was scanned. PFOODR excitation signals associated with transitions into triplet states were detected by selectively monitoring violet fluorescence to the $a\,^3\Sigma_u^+$ and/or $b\,^3\Pi_u$ states with a system consisting of various filters (Kopp 4-96+5-56+5-57), a photomultiplier tube (PMT) (Hamamatsu R928), and a lock-in amplifier.

III. HYPERFINE COUPLING SCHEMES AND HAMILTONIAN

$^6Li^7Li$ is interesting because it can be considered homonuclear with regard to Coulomb interactions but heteronuclear with regard to nuclear spin hyperfine interactions. The nuclear spins for ^6Li and ^7Li are 1 and 3/2, respectively. The coupling strengths between nuclear spin and electronic angular momenta are different for ^6Li and ^7Li. The hyperfine coupling scheme for $^7Li_2$ is case $b_{\beta S}$, and is illustrated in Fig. 1(a). In this case, the Fermi contact interactions between the electron spin **S** and each of the nuclear spins $\mathbf{I}_7$ are identical. Thus we may write $\mathbf{H}^{\text{Fermi contact}} = b\mathbf{I}_7\cdot\mathbf{S} + b\mathbf{I}_7\cdot\mathbf{S} = b\mathbf{I}\cdot\mathbf{S}$, where we represent the vector sum of the two nuclear spins $\mathbf{I}_7$ and $\mathbf{I}_7$ as **I** ($\mathbf{I}_7+\mathbf{I}_7=\mathbf{I}$). Due to this Fermi contact interaction **I** couples with **S** to form **G**, and the energies of the *G* components can be calculated from Eq. (1).

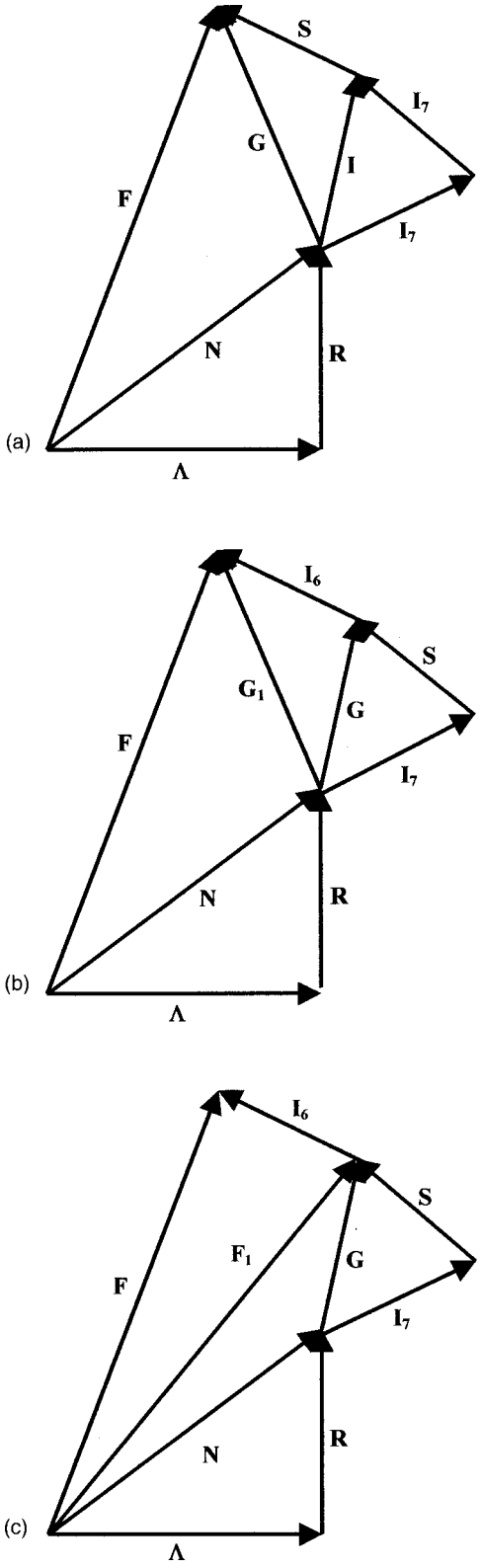

FIG. 1. Possible hyperfine coupling schemes for $^7Li_2$ and $^6Li^7Li$ triplet Rydberg states.

The $^6Li^7Li$ triplet states could also follow a subcase of coupling case $b_{\beta S}$ similar to that of the $^7Li_2$ triplets. This would be represented by Fig. 1(a) with one of the $\mathbf{I}_7$'s replaced by $\mathbf{I}_6$ ($\mathbf{I}=\mathbf{I}_6+\mathbf{I}_7, \mathbf{G}=\mathbf{I}+\mathbf{S}, \mathbf{F}=\mathbf{G}+\mathbf{N}$). However, in the case of $^7Li_2$, the Fermi contact interactions for the two

Downloaded 25 Aug 2002 to 128.180.23.36. Redistribution subject to AIP license or copyright, see http://ojps.aip.org/jcpo/jcpcr.jsp

nuclei are identical. For $^6Li^7Li$, the Fermi contact interaction of the ^6Li nucleus is weaker than that of the ^7Li nucleus. Thus the Fermi contact interaction cannot be treated in the same manner as for $^7Li_2$ (i.e., $\mathbf{H}^{\text{Fermi contact}} = b_7\mathbf{I}_7\cdot\mathbf{S} + b_6\mathbf{I}_6\cdot\mathbf{S} \neq b_{\text{effective}}\mathbf{I}\cdot\mathbf{S}$). In this case, the two nuclear spins in $^6Li^7Li$ would couple as in Fig. 1(a) only if the magnetic dipole interaction, $\mathbf{I}_7\cdot\mathbf{I}_6$, is stronger than all other nuclear spin interactions, including the Fermi contact interaction, for a particular N level. Since that situation is unlikely, we must consider the alternative hyperfine coupling schemes of Figs. 1(b) and 1(c) to describe the triplet states of $^6Li^7Li$. In Fig. 1(b), the ^7Li nuclear spin, $\mathbf{I}_7$, first couples with the electronic spin, $\mathbf{S}$, to give $\mathbf{G}$. $\mathbf{G}$ then couples with the ^6Li nuclear spin, $\mathbf{I}_6$, to give $\mathbf{G}_1$, and $\mathbf{G}_1$ in turn couples to $\mathbf{N}$ to give $\mathbf{F}$. In Fig. 1(c), the ^7Li nuclear spin couples with the electronic spin to give $\mathbf{G}$. $\mathbf{G}$ then couples with $\mathbf{N}$ to give $\mathbf{F}_1$, and finally, the ^6Li nuclear spin couples to $\mathbf{F}_1$ to give the total angular momentum $\mathbf{F}$. The actual coupling of a particular $^6Li^7Li$ electronic state need not be in one of these pure limiting cases, but rather in an intermediate case.

The effective Hamiltonian within a particular vibrational level of a $^6Li^7Li$ electronic state can be written as

$$\mathbf{H} = \mathbf{H}^{\text{rot}} + \mathbf{H}^{\text{so}} + \mathbf{H}^{\text{ss}} + \mathbf{H}^{\text{sr}} + \mathbf{H}^{\text{hfs}}, \tag{2}$$

$$\mathbf{H}^{\text{rot}} = B\mathbf{N}^2 - D\mathbf{N}^4,$$

rotational and centrifugal distortion energy, (3)

$$\mathbf{H}^{\text{so}} = A\mathbf{L}\cdot\mathbf{S}, \text{spin–orbit interaction}, \tag{4}$$

$$\mathbf{H}^{\text{ss}} = \tfrac{2}{3}\lambda(3\mathbf{S}_z^2 - \mathbf{S}^2), \text{spin–spin interaction}, \tag{5}$$

$$\mathbf{H}^{\text{sr}} = \gamma\mathbf{N}\cdot\mathbf{S}, \text{spin–rotation interaction}. \tag{6}$$

Matrix elements of the rotational, centrifugal distortion, spin–orbit, spin–spin, and spin–rotation interactions can be found in Kovacs.[13] The triplet states of $^6Li^7Li$ have nonzero electronic spin, so the magnetic dipole terms will be the dominant hyperfine interaction. The magnetic hyperfine interaction Hamiltonian is given by[14]

$$\mathbf{H}^{\text{hfs}} = \mathbf{H}^{\text{hfs,7}} + \mathbf{H}^{\text{hfs,6}}, \tag{7}$$

where

$$\mathbf{H}^{\text{hfs,7}} = a_7\mathbf{I}_7\cdot\mathbf{L} + b_7\mathbf{I}_7\cdot\mathbf{S} + \tfrac{1}{3}c_7(3I_{7z}S_z - \mathbf{I}_7\cdot\mathbf{S}), \tag{8}$$

and

$$\mathbf{H}^{\text{hfs,6}} = a_6\mathbf{I}_6\cdot\mathbf{L} + b_6\mathbf{I}_6\cdot\mathbf{S} + \tfrac{1}{3}c_6(3I_{6z}S_z - \mathbf{I}_6\cdot\mathbf{S}). \tag{9}$$

Here I_7 and I_6 identify the nuclear spins of ^7Li and ^6Li, respectively, and a_7, b_7, c_7 and a_6, b_6, c_6 stand for the hyperfine interaction parameters of the ^7Li nucleus and ^6Li nucleus, respectively. The hyperfine constants are defined by

$$a = g_S g_N \mu_B \mu_N \sum_i \left\langle \frac{1}{r_i^3} \right\rangle_{\text{ave}}, \tag{10}$$

$$b = \frac{8\pi}{3} g_S g_N \mu_B \mu_N \sum_i \langle \Psi_i^2(r_i = 0) \rangle_{\text{ave}}, \tag{11}$$

and

$$c = \frac{3}{2} g_S g_N \mu_B \mu_N \sum_i \left\langle \frac{3\cos^2\theta_i - 1}{r_i^3} \right\rangle_{\text{ave}}. \tag{12}$$

In these expressions μ_B and μ_N are the Bohr and nuclear magnetons, $g_S (g_S = 2.0023)$ and g_N are the electron spin g- and nuclear spin g-factors, respectively, and r_i, θ_i are the spherical polar coordinates of electron i, defined with respect to the nucleus under consideration and the internuclear axis. The term $a\mathbf{I}\cdot\mathbf{L}$ represents the nuclear spin–electron orbital angular momentum interaction, $b\mathbf{I}\cdot\mathbf{S}$ represents the Fermi contact interaction, and the c term represents the dipolar electron spin–nuclear spin interaction. $\Psi_i^2(r_i = 0)$ is the electron spin density at the nucleus. The average is over all electrons in the molecule. If the angular momenta of a group of electrons add vectorially to a resultant angular momentum of zero, as in the case of a closed shell, then their contribution to the average magnetic field at the nucleus is zero. Hence it is necessary to take into account only the electrons in unfilled orbitals. Hyperfine splitting is particularly important and large for σ orbitals, since they penetrate most closely to the nucleus (there is no nodal plane that includes the internuclear axis). In this case, the Fermi contact term will most likely dominate the hyperfine structure.

We have worked out the magnetic dipole hyperfine interaction matrix elements using basis functions appropriate to the coupling case of Fig. 1(c). In this basis, the electronic orbital–nuclear spin interaction matrix elements are

$$\langle \Lambda S I_7 G' N' F_1' I_6 F | a_7\mathbf{I}_7\cdot\mathbf{L} | \Lambda S I_7 G N F_1 I_6 F \rangle$$
$$= a_7\Lambda(-1)^{N+G+F_1+I_7+S+G+I+N'-\Lambda}\delta_{F_1'F_1}\sqrt{I_7(I_7+1)(2I_7+1)(2G+1)(2G'+1)(2N+1)(2N'+1)}$$
$$\times \begin{Bmatrix} F_1 & G & N \\ 1 & N' & G' \end{Bmatrix} \begin{Bmatrix} S & G & I_7 \\ 1 & I_7 & G' \end{Bmatrix} \begin{pmatrix} N' & 1 & N \\ -\Lambda & 0 & \Lambda \end{pmatrix}, \tag{13}$$

$$\langle \Lambda S I_7 G' N' F_1' I_6 F | a_6\mathbf{I}_6\cdot\mathbf{L} | \Lambda S I_7 G N F_1 I_6 F \rangle$$
$$= a_6\Lambda(-1)^{I_6+F+2F_1'+N+G+1+N'-\Lambda}\delta_{GG'}\sqrt{I_6(I_6+1)(2I_6+1)(2F_1+1)(2F_1'+1)(2N+1)(2N'+1)}$$
$$\times \begin{Bmatrix} F & I_6 & F_1' \\ 1 & F_1 & I_6 \end{Bmatrix} \begin{Bmatrix} N' & F_1' & G \\ F_1 & N & 1 \end{Bmatrix} \begin{pmatrix} N' & 1 & N \\ -\Lambda & 0 & \Lambda \end{pmatrix}. \tag{14}$$

The Fermi-contact interaction matrix element of the ^7Li nucleus is

Downloaded 25 Aug 2002 to 128.180.23.36. Redistribution subject to AIP license or copyright, see http://ojps.aip.org/jcpo/jcpcr.jsp

$$\langle \Lambda S I_7 G' N' F_1' I_6 F | b_7 \mathbf{I}_7 \cdot \mathbf{S} | \Lambda S I_7 G N F_1 I_6 F \rangle = \frac{b_7}{2} \delta_{GG'} \delta_{N'N} \delta_{F_1 F_1'} [G(G+1) - I_7(I_7+1) - S(S+1)], \tag{15}$$

and the Fermi contact interaction matrix element of the ^{6}Li nucleus is

$$\begin{aligned}
&\langle \Lambda S I_7 G' N' F_1' I_6 F | b_6 \mathbf{I}_6 \cdot \mathbf{S} | \Lambda S I_7 G N F_1 I_6 F \rangle \\
&= b_6 (-1)^{I_7 + I_6 + F + 2F_1' + N + G + G' + S} \delta_{NN'} \sqrt{I_6(I_6+1)(2I_6+1)(2F_1+1)(2F_1'+1)(2G+1)(2G'+1)S(S+1)(2S+1)} \\
&\quad \times \begin{Bmatrix} F & F_1' & I_6 \\ 1 & I_6 & F_1 \end{Bmatrix} \begin{Bmatrix} G' & F_1' & N \\ F_1 & G & 1 \end{Bmatrix} \begin{Bmatrix} S & G' & I_7 \\ G & S & 1 \end{Bmatrix}.
\end{aligned} \tag{16}$$

The electronic spin–nuclear spin dipolar interaction matrix elements are

$$\begin{aligned}
&\langle \Lambda S I_7 G' N' F_1' I_6 F | c_7 I_{7z} S_z | \Lambda S I_7 G N F_1 I_6 F \rangle \\
&= c_7 \frac{\sqrt{30}}{3} (-1)^{N + G' + F_1 + N' - \Lambda} \delta_{F_1 F_1'} \sqrt{I_7(I_7+1)(2I_7+1)(2G+1)(2G'+1)S(S+1)(2S+1)(2N+1)(2N'+1)} \\
&\quad \times \begin{Bmatrix} F_1 & G' & N' \\ 2 & N & G \end{Bmatrix} \begin{Bmatrix} S & S & 1 \\ I_7 & I_7 & 1 \\ G' & G & 2 \end{Bmatrix} \begin{Bmatrix} S & G & I_7 \\ G' & S & 1 \end{Bmatrix} \begin{pmatrix} N' & 2 & N \\ -\Lambda & 0 & \Lambda \end{pmatrix},
\end{aligned} \tag{17}$$

and

$$\begin{aligned}
&\langle \Lambda S I_7 G' N' F_1' I_6 F | c_6 I_{6z} S_z | \Lambda S I_7 G N F_1 I_6 F \rangle \\
&= c_6 \frac{\sqrt{30}}{3} (-1)^{I_6 + F_1' + F + I_7 + S + G' + N' - \Lambda} \\
&\quad \times \sqrt{I_6(I_6+1)(2I_6+1)(2F_1'+1)(2F_1+1)(2G'+1)(2G+1)S(S+1)(2S+1)(2N+1)(2N'+1)} \\
&\quad \times \begin{Bmatrix} F_1 & I_6 & F \\ I_6 & F_1' & 1 \end{Bmatrix} \begin{Bmatrix} G & G' & 1 \\ N & N' & 2 \\ F_1 & F_1' & 1 \end{Bmatrix} \begin{Bmatrix} S & G & I_7 \\ G' & S & 1 \end{Bmatrix} \begin{pmatrix} N' & 2 & N \\ -\Lambda & 0 & \Lambda \end{pmatrix}.
\end{aligned} \tag{18}$$

In these expressions, the brackets

$$\begin{pmatrix} \cdot & \cdot & \cdot \\ \cdot & \cdot & \cdot \end{pmatrix}, \begin{Bmatrix} \cdot & \cdot & \cdot \\ \cdot & \cdot & \cdot \end{Bmatrix}, \text{ and } \begin{Bmatrix} \cdot & \cdot & \cdot \\ \cdot & \cdot & \cdot \\ \cdot & \cdot & \cdot \end{Bmatrix}$$

represent 3-j, 6-j and 9-j symbols, respectively.

Diagonalization of the full Hamiltonian matrix, including all terms listed in Eq. (2), yields the energies of hyperfine levels in intermediate as well as limiting case coupling schemes. Here we report the full set of magnetic dipole matrix elements evaluated in the Fig. 1(c) basis as an aid to future workers when higher resolution spectra become available. However, for our purposes it appears that terms involving the ^{6}Li nuclear spin, as well as the electron orbital–nuclear spin and electron spin–nuclear spin dipolar interactions of the ^{7}Li nucleus do not contribute to structure we are able to resolve with our current experimental setup (see Results).

IV. RESULTS

The energy separation between the $A\,^1\Sigma_u^+$ ($v_A'=5$, $J'=24$) and $b\,^3\Pi_u$ ($v_b'=12$, $N'=23$, $J'=24$) mixed levels is 0.225 cm^{-1}.[10] The Doppler linewidth (FWHM) of ^{6}Li^{7}Li transitions at 1000 K is about 0.1 cm^{-1}. Thus, when the *pump* laser is held fixed to the center of the Doppler profile of the $b\,^3\Pi_u$ ($v_b'=12$, $N'=23$, $J'=24$)$\leftarrow X\,^1\Sigma_g^+$ ($v''=0$, $J''=23$ or 25) transition, not only does it excite all hyperfine components of the $b\,^3\Pi_u$ ($v_b'=12$, $N'=23$, $J'=24$) level (different velocity projections along the laser propagation direction are resonant with the *pump* laser for each of the different hyperfine components), but also it simultaneously excites the $A\,^1\Sigma_u^+$ ($v_A'=5$, $J'=24$) level. It has been shown in Refs. 5, 6, and 15 that when the *pump* and *probe* lasers co-propagate, the hyperfine structures of both the intermediate and upper levels contribute to the observed structure of the *probe* laser excitation spectrum. However, when the *pump* and *probe* lasers have comparable frequencies and counter-propagate through the vapor, as in the present experiment, then the Doppler shifts from the two lasers mostly cancel, and the observed splittings of the OODR excitation lines reflect the hyperfine structure of the upper triplet Rydberg states only.[15]

A. The $3\,^3\Sigma_g^+$ state

The Li_2 $3\,^3\Sigma_g^+$ state has the electronic configuration $[\sigma_g(2s)]^1[(4s)\sigma_g]^1$. The $^6Li_2$ $3\,^3\Sigma_g^+$ state was first observed by CW PFOODR excitation spectroscopy.[16] No HFS

Downloaded 25 Aug 2002 to 128.180.23.36. Redistribution subject to AIP license or copyright, see http://ojps.aip.org/jcpo/jcpcr.jsp

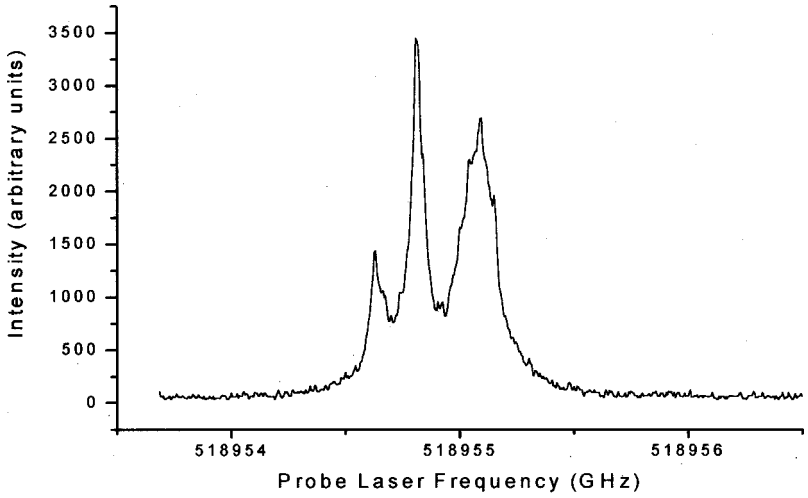

FIG. 2. The splitting of the $3\,^3\Sigma_g^+$ ($v=6$, $N=23$) $\leftarrow b\,^3\Pi_u$ ($v_b'=12$, $N'=23$, $J'=24$) PFOODR hypermultiplet. The probe laser power was reduced to ~1 mW in order to reduce power broadening.

was resolved. The $^7Li_2$ $3\,^3\Sigma_g^+$ state was observed by CW PFOODR excitation with resolved HFS.[5] Using the accurately calculable reduced masses for the three $^6Li_2$, $^7Li_2$, and $^6Li^7Li$ isotopomers, the term values of the $^6Li^7Li$ $3\,^3\Sigma_g^+$ vibronic levels can be calculated from the $3\,^3\Sigma_g^+$ state constants of $^6Li_2$ or $^7Li_2$. Five vibrational levels, $v=3-7$, of the $^6Li^7Li$ $3\,^3\Sigma_g^+$ state have been observed.[11] Transitions from a single $b\,^3\Pi_u(v_b', N', J'=N'+1)$ level into one $3\,^3\Sigma_g^+$ vibrational level should consist of two rotational lines ($N=N'+2\leftarrow N'$ and $N=N'\leftarrow N'$), but only the $N=N'\leftarrow N'$ component was observed in our spectra. The $N=N'+2\leftarrow N'$ line is predicted to be almost 4 orders of magnitude weaker than the $N=N'\leftarrow N'$ line according to intensity calculations.[13]

The PFOODR excitation line into the $^6Li^7Li$ $3\,^3\Sigma_g^+$ ($v=6$, $N=23$) level is shown in Fig. 2. Observed transitions into the $N=23$ level of other vibrational states show the same hyperfine splitting. The spectrum contains three main components. The weak component at lowest frequency consists of two partially resolved peaks. The middle component is narrower and displays no resolvable structure. The component at highest frequency is broader and exhibits unresolved structure.

From the free atom values we know that the Fermi contact interaction of the ^7Li nucleus is much stronger than that of the ^6Li nucleus. Therefore the hyperfine splitting will be dominated by the Fermi contact interaction of the ^7Li nucleus if either coupling scheme, shown in Figs. 1(b) or 1(c) are valid. In either of these cases $I_7=3/2$, $S=1$, and therefore $G=5/2$, 3/2, 1/2, and the energies can be calculated from the expression

$$\Delta E(G+1, G)=E(G+1, I_7, S)-E(G, I_7, S)$$
$$=b_7(G+1). \tag{19}$$

The main component splittings are therefore predicted to be $(5/2)b_7$ and $(3/2)b_7$. The measured separations are 0.278 GHz and 0.167 GHz, respectively, and the ratio of the separations (1.66) agrees well with this prediction. The absolute magnitude of the splittings yields $b_7=111$ MHz for the Fermi contact constant of the interaction between the ^7Li nucleus and the electronic spin, in good agreement with a simple prediction based on the Fermi contact constant of the ^7Li ground state atom (see Discussion).

Alternatively, we note that the nuclear spins of ^6Li and ^7Li are 1 and 3/2, respectively. Thus if the hyperfine coupling scheme is that of Fig. 1(a), then we should still observe 3 main components ($I=5/2$, 3/2, and 1/2) and the splittings should be 5/2 and 3/2 times the $\mathbf{I_7}\cdot\mathbf{I_6}$ interaction constant. However, for this scheme to be valid, the $\mathbf{I_7}\cdot\mathbf{I_6}$ interaction must be much stronger than the $\mathbf{I_7}\cdot\mathbf{S}$ Fermi contact interaction. On theoretical grounds, we believe this is unlikely {the $\mathbf{I_7}\cdot\mathbf{I_6}$ interaction strength should be comparable to the dipolar electron spin–nuclear spin interaction [the "*c* term" in Eqs. (8) and (9)] which we know is negligible}. Moreover, in this Fig. 1(a) coupling scheme, the primary splittings (due to the $\mathbf{I}_7\cdot\mathbf{I}_6$ interaction) should be much larger than those predicted from the $\mathbf{I_7}\cdot\mathbf{S}$ Fermi contact term. Since we have just demonstrated that the primary splittings are consistent with the Fermi contact interaction, we reject the coupling scheme of Fig. 1(a).

Now the question is: which of the remaining coupling cases, Figs. 1(b) or 1(c), best describes the coupling for the $^6Li^7Li$ $3\,^3\Sigma_g^+$ state? If $\mathbf{I_6}$ couples to $\mathbf{G}$ ($\mathbf{G}=\mathbf{I_7}+\mathbf{S}$) before $\mathbf{N}$ [Fig. 1(b)], the $\mathbf{G_1}$ components will exhibit the splittings,

$G=1/2$, $I_6=1$, $G_1=3/2$, 1/2,

$G=3/2$, $I_6=1$, $G_1=5/2$, 3/2, 1/2,

$G=5/2$, $I_6=1$, $G_1=7/2$, 5/2, 3/2.

However, if $\mathbf{N}$ couples to $\mathbf{G}$ before $\mathbf{I_6}$ [Fig. 1(c)], the $\mathbf{F_1}$ components will split according to the following scheme:

$G=1/2$, $F_1=N+1/2$, $N-1/2$,

$G=3/2$, $F_1=N+3/2$, $N+1/2$, $N-1/2$, $N-3/2$,

$G=5/2$, $F_1=N+5/2$, $N+3/2$, $N+1/2$, $N-1/2$,

$N-3/2$, $N-5/2$.

In Fig. 2, the $G=1/2$ peak splits into two partially resolved components; the $G=3/2$ peak exhibits no resolvable splitting; and the $G=5/2$ peak exhibits 5 slightly resolved com-

Downloaded 25 Aug 2002 to 128.180.23.36. Redistribution subject to AIP license or copyright, see http://ojps.aip.org/jcpo/jcpcr.jsp

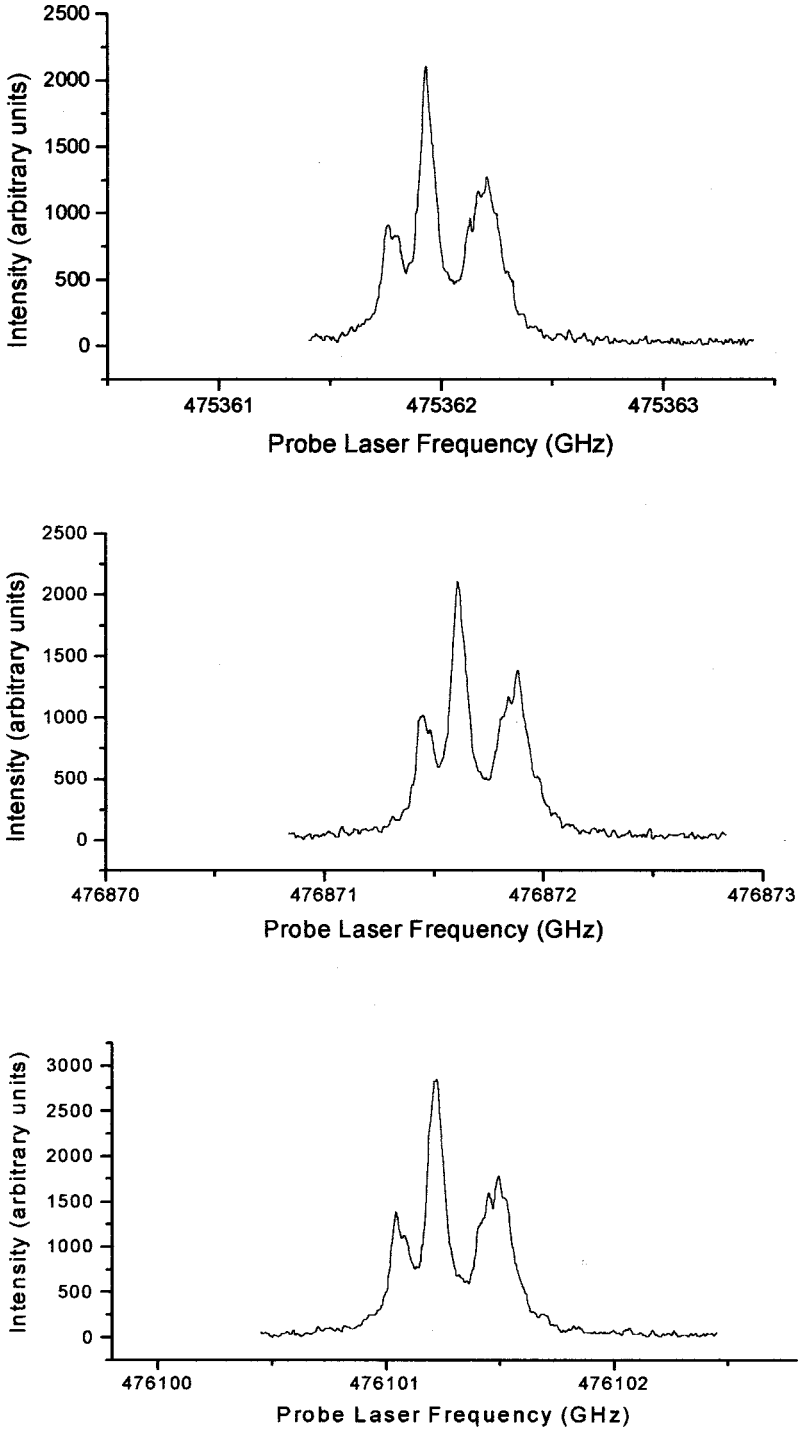

FIG. 3. The splitting of the $1\,^3\Delta_g$ $(v=4, N=22, 23, 24) \leftarrow b\,^3\Pi_u$ $(v'_b=12, N'=23, J'=24)$ PFOODR hypermultiplet. The probe laser power was reduced to ~1 mW in order to reduce power broadening.

ponents. These components do not appear to be noise as they were always present when we repeated the scan many times. This suggests that the $3\,^3\Sigma_g^+$ state follows the coupling case shown in Fig. 1(c) rather than that shown in Fig. 1(b) since the Fig. 1(b) coupling scheme yields only 3 components within the $G=5/2$ peak. Our attempts to obtain the spin–spin, spin–rotation, and/or the ^{6}Li Fermi contact parameters from simulations of the current spectra have failed because this substructure is not sufficiently well resolved. However, the Fermi contact constant for the ^{6}Li nucleus in the $^6Li^7Li$ molecule triplet Rydberg states can be estimated to be $\frac{1}{4}$ of the Fermi contact constant of the ^{6}Li atomic ground state, i.e., $b_6 \approx 38$ MHz.

B. The $1\,^3\Delta_g$ state

The $1\,^3\Delta_g$ state of $^6Li_2$ was observed by Xie and Field with sub-Doppler resolution.[16] No HFS was resolved. The $1\,^3\Delta_g$ state of $^7Li_2$ was observed by sub-Doppler, CW, PFOODR excitation spectroscopy with resolved HFS.[4,17] Transitions from an intermediate $b\,^3\Pi_u$ level into the $1\,^3\Delta_g$ state consist of $\Delta N=\Delta J=0, \pm 1$ Q, P, and R lines. The term values of the $1\,^3\Delta_g$ levels of $^6Li^7Li$ can be calculated from the $^6Li_2$ or $^7Li_2$ constants. Three vibrational levels, $v=2-4$, have been observed with resolved HFS.

Figure 3 shows transitions to the three rotational levels, $N=22$, 23, and 24 of the $^6Li^7Li$ $1\,^3\Delta_g$ $v=4$ vibrational

Downloaded 25 Aug 2002 to 128.180.23.36. Redistribution subject to AIP license or copyright, see http://ojps.aip.org/jcpo/jcpcr.jsp

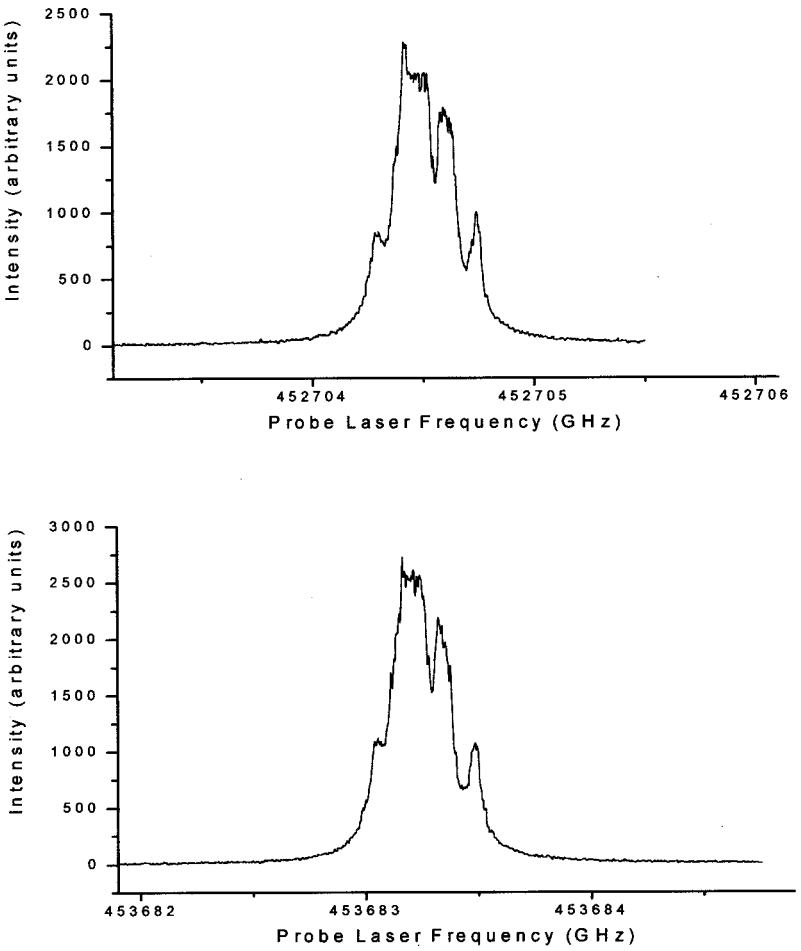

FIG. 4. The hyperfine splitting of the $2\,^3\Pi_g$ ($v=4$, $N=22,\ 24$) $\leftarrow b\,^3\Pi_u$ ($v_b'=12,\ N'=23,\ J'=24$) PFOODR hypermultiplet. The probe laser power was reduced to ~1 mW in order to reduce power broadening.

level. The three lines exhibit the same basic hyperfine structure as the $3\,^3\Sigma_g^+$ lines; each rotational line splits coarsely into three components; the one at lowest frequency has two partially resolved components; the middle one is narrower and exhibits no splitting; the one at highest frequency has 5 partially resolved components. The Fermi contact constant of the ^{7}Li nucleus, $b_7=107$ MHz, has been calculated from the measured intervals. The Fermi contact constant of the ^{6}Li nucleus, b_6, and other small parameters, could not be determined at our resolution.

C. The $2\,^3\Pi_g$ state

The $2\,^3\Pi_g$ state of $^6Li_2$ and $^7Li_2$ was observed by sub-Doppler, CW PFOODR spectroscopy.[16,18] The $2\,^3\Pi_g$ state dissociates adiabatically to the $2p+2p$ atomic limit. *Ab initio* calculations show that its electronic configuration changes with internuclear distance: at small R, it is a Rydberg state; at $R\approx R_e$, it has 60% Rydberg character; at larger internuclear distance, $R\approx\infty$, it becomes a doubly excited state.[18]

The HFS of the $^7Li_2$ $2\,^3\Pi_g$ state has been resolved.[6] The Fermi contact constant of this $2\,^3\Pi_g$ state is 60 MHz, rather than 100 MHz as found for the $^3\Delta_g$, $^3\Sigma_g^+$, $3\,^3\Pi_g$, and $b\,^3\Pi_u$ states. The smaller value of the Fermi contact constant reflects the $[\sigma_u(np)]^1[\pi_u(np)]^1$ doubly excited character of the $2\,^3\Pi_g$ state. The pure doubly excited state, $1\,^3\Sigma_g^-$, belongs to the $[\pi_u(np)]^1[\pi_u(np)]^1$ configuration and its HFS is not resolvable with sub-Doppler resolution in a heatpipe oven.

Electronic transitions from a case (b) $b\,^3\Pi_u$ intermediate level to a particular vibrational level of a case (b) $2\,^3\Pi_g$ state consist of P and R lines and a weak Q line. In our PFOODR excitation spectra of $^6Li^7Li$, the Q line is about 250 times weaker than the P and R lines. Figure 4 shows the HFS of the $2\,^3\Pi_g$ $v=4$, $N=22$ and 24 levels. The hyperfine splitting pattern of these lines is quite different from those of the $3\,^3\Sigma_g^+$ and $1\,^3\Delta_g$ states. We cannot offer an explanation of these $^6Li^7Li$ $2\,^3\Pi_g$ state hyperfine splittings at the present time.

V. DISCUSSION

As we have pointed out, the dominant hyperfine interaction of $^7Li_2$ triplet states is the Fermi contact interaction. Li Li *et al.*[1] estimated the Fermi contact constants of the triplet Rydberg states of H_2, $^7Li_2$, and Na_2, which are all built on the $M_2^+\,X\,^2\Sigma_g^+$ ion-core ground state with electronic configuration $[\sigma_g(ns)]^1$ ($n=1$, 2, and 3 for H_2, $^7Li_2$, and Na_2, respectively). To do so they used a simple model assuming that the $\sigma_g(ns)$ molecular orbital is given by the primitive linear combination of atomic orbitals (LCAO), $(2)^{-1/2}[|ns_A\rangle+|ns_B\rangle]$. They predicted that the Fermi contact interaction constants, b, for all H_2, $^7Li_2$, and Na_2 triplet

Downloaded 25 Aug 2002 to 128.180.23.36. Redistribution subject to AIP license or copyright, see http://ojps.aip.org/jcpo/jcpcr.jsp

Rydberg states are $\sim\frac{1}{4}$ the value of the Fermi contact constant of the corresponding atomic $ns\,^2S$ ground state. A factor of $\frac{1}{2}$ from the normalization of the $\sigma_g(ns)$ valence molecular orbital [the probability of finding the electron at nucleus 1 in $\sigma_g(ns)$ is half that of finding it at the free atom nucleus in the $ns\,^2S$ state] and another factor of $\frac{1}{2}$ due to the fact that only one of the two $s=\frac{1}{2}$ electrons that make up the total electron spin $S=1$ in the molecule occupies a given spin–orbital, combine to produce the overall factor of 1/4. The agreement between observed b values ($\sim$100 MHz for $^7Li_2$ and 210–220 MHz for Na_2) and the predicted b values (101 MHz for $^7Li_2$ and 221 MHz for Na_2) is quite good for $^7Li_2$ and Na_2 and slightly worse for H_2 (where the predicted b value is 355 MHz and the observed value is 450 MHz).[19,20]

For a heteronuclear molecule (for example different isotopomers and mixed alkali diatomics), however, the situation is different. The Fermi contact interaction of the ^7Li nucleus is stronger than that of the ^6Li nucleus by a factor of 2.6. In $^6Li^7Li$ triplet states, the Fermi contact interaction of the ^7Li nucleus should be the same as that for the corresponding triplet state of the $^7Li_2$ isotopomer because the electronic wave functions of different isotopomers are nearly identical. In other words, the density of the $[\sigma_g(2s)]$ valence orbital at the ^7Li nucleus in $^6Li^7Li$ should be the same as it is in $^7Li_2$ for the same electronic state. The Fermi contact interaction of the ^6Li nucleus in the $^6Li^7Li$ triplet states is weaker than that of the ^7Li nucleus and the hyperfine splitting is therefore dominated by the Fermi contact interaction of the ^7Li nucleus. More importantly, in $^7Li_2$ the Fermi contact interactions of the two nuclei are identical and the coupling scheme of Fig. 1(a) must be used. For $^6Li^7Li$ triplet states, either the coupling scheme of Fig. 1(b) or that of Fig. 1(c) is valid. In either case the HFS patterns will be quite different from those of $^7Li_2$.

The hyperfine interaction scheme for the $^6Li^7Li$ triplet states is very similar to the HFS exhibited by the NaK $4\,^3\Sigma^+$ state.[21] Other NaK triplet states follow case $b_{\beta J}$ coupling.[15,22–26] However, for all NaK triplet states studied so far, the Fermi contact interaction of the Na nucleus plays the dominant role. The Fermi contact interaction of the Na nucleus in NaK, however, is larger than that in the Na_2 triplet Rydberg states: in NaK $b_{Na}=333$ MHz; in Na_2, $b_{Na}=220$ MHz. This means that in those NaK triplet Rydberg states studied so far the density of the σ valence orbital at the Na nucleus is not only higher than that at the K nucleus, but higher than that in the Na_2 triplet Rydberg states.

When more than one σ valence orbital is singly occupied, the Fermi contact interaction will be stronger than that of the $X\,^2\Sigma_g^+$-core triplet Rydberg states. The $a\,^3\Sigma_u^+$ state of Na_2 is a repulsive state with a shallow well at $R_e=5.09$ Å.[27] It has the configuration $[\sigma_g 3s]^1[\sigma_u 3s]^1$. The Fermi contact constant of the $a\,^3\Sigma_u^+$ state is 293 MHz,[28] rather than 220 MHz, because it has two unpaired electrons in σ orbitals, one in σ_g and one in σ_u. The $a\,^3\Sigma^+$ state of NaK also has a larger Fermi contact constant, 420 MHz,[29,30] compared to 330 MHz found for the NaK triplet Rydberg states.

When a Rydberg state is ionized, a ground state ion forms. The ion ground state, $X\,^2\Sigma_g^+$, only has *one valence* $\sigma_g(ns)$ *electron*. The factor of 1/2 (only one of the two $s=1/2$ electrons that make up the total electron spin $S=1$ in the molecule occupies a given spin–orbital for Rydberg states) no longer applies. Thus a Fermi contact constant that is a factor of 2 larger than that for the triplet Rydberg states is expected for the ground state ions. This has indeed been found to be the case by observation of the hyperfine constant of H_2^+; the Fermi contact constant of H_2^+ is 923 MHz,[31] while that of the triplet Rydberg states is 450 MHz.

VI. CONCLUSIONS

Hyperfine structure of the $^6Li^7Li$ $1\,^3\Delta_g$, $2\,^3\Pi_g$, and $3\,^3\Sigma_g^+$ states has been resolved and analyzed. The hyperfine splitting of the $1\,^3\Delta_g$ and $3\,^3\Sigma_g^+$ states arises predominantly from the Fermi contact interaction between the ^7Li nuclear spin and the $\sigma_g(2s)$ valence electron. The Fermi contact constants of the $3\,^3\Sigma_g^+$ and $1\,^3\Delta_g$ states are $b_7=110$ and 107 MHz, respectively. Additional splittings due to the spin–spin, spin–rotation, and/or Fermi contact interaction of the ^6Li nucleus were not resolved. The $2\,^3\Pi_g$ state exhibits a different coupling scheme due to its doubly excited character.

The Fermi contact interactions in homonuclear alkali molecules, different isotopomers, and heteronuclear alkali diatomics have been discussed. For different isotopomers, the electronic wave functions of corresponding states are nearly identical. The Fermi contact interaction of each nucleus is the same as in its homonuclear dimer. In a heteronuclear molecule like NaK the valence σ orbital is essentially different than in Na_2 or K_2. For NaK, there should be complementary pairs of states with one member of each pair having its valence σ orbital polarized towards the Na nucleus and the other having its valence σ orbital polarized towards the K nucleus. For the first type, the Fermi contact term involving the Na nucleus dominates the hyperfine structure, but the Fermi contact constant is larger than that in Na_2.

Finally, when the two unpaired electrons occupy two σ valence orbitals, as for example in the Na_2 $a\,^3\Sigma_u^+$ state, the Fermi contact interaction is stronger than in the case where only one σ valence orbital is singly occupied. A ground state ion, however, has twice the Fermi contact constant as the Rydberg states because in the former case the Rydberg electron is not present to reduce the Fermi contact interaction constant by a factor of 2.

ACKNOWLEDGMENTS

The authors would like to thank Dr. A. Peet Hickman for valuable discussions on this topic and Jenny Magnes for technical assistance. Support from the NSF (PHY9983533) in the U.S. and from the NNSF (19804008 and 29973020) and NKBRSF in China is gratefully acknowledged. Li Li thanks the Lagerqvist Research Fund of Temple University for support during her visit.

[1] Li Li, Q. Zhu, and R. W. Field, J. Mol. Spectrosc. **134**, 50 (1989).
[2] Li Li, Q. Zhu, and R. W. Field, Mol. Phys. **66**, 685 (1989).
[3] Y. Liu, B. Ji, A. S-C. Cheung, W. C. Stwalley, R. W. Field, A. M. Lyyra, and Li Li, J. Chem. Phys. **115**, 3647 (2001), and references therein.
[4] Li Li, T. An, T.-J. Whang, A. M. Lyyra, W. C. Stwalley, R. W. Field, and R. A. Bernheim, J. Chem. Phys. **96**, 3342 (1992).

Downloaded 25 Aug 2002 to 128.180.23.36. Redistribution subject to AIP license or copyright, see http://ojps.aip.org/jcpo/jcpcr.jsp

[5] A. Yiannopoulou, K. Urbanski, A. M. Lyyra, Li Li, B. Ji, J. T. Bahns, and W. C. Stwalley, J. Chem. Phys. **102**, 3024 (1995).
[6] Li Li, A. Yiannopoulou, K. Urbanski, A. M. Lyyra, B. Ji, W. C. Stwalley, and T. An, J. Chem. Phys. **105**, 6192 (1996).
[7] Li Li, A. Yiannopoulou, K. Urbanski, A. M. Lyyra, B. Ji, W. C. Stwalley, and T. An, J. Korean Phys. Soc. **32**, 309 (1998).
[8] Li Li and A. M. Lyyra, Spectrochim. Acta, Part A **55A**, 2147 (1999).
[9] G. Lazarov, A. M. Lyyra, Li Li, and J. Huennekens, J. Mol. Spectrosc. **196**, 259 (1999).
[10] P. Yi, M. Song, Y. Liu, A. M. Lyyra, and Li Li, Chem. Phys. Lett. **349**, 426 (2001).
[11] A. Lazoudis, P. Yi, Li Li, and A. M. Lyyra, J. Mol. Spectrosc. (to be submitted).
[12] A. N. Nesmeyanov, *Vapour Pressure of the Chemical Elements*, edited by Robert Gray (Elsevier, Amsterdam, 1963).
[13] I. Kovacs, *Rotational Structure in the Spectra of Diatomic Molecules* (American Elsevier, New York, 1969).
[14] C. H. Townes and A. L. Schawlow, *Microwave Spectroscopy* (McGraw–Hill, New York, 1955).
[15] J. Huennekens, I. Prodan, A. Marks, L. Sibbach, E. Galle, T. Morgus, and Li Li, J. Chem. Phys. **113**, 7384 (2000).
[16] X. Xie and R. W. Field, J. Mol. Spectrosc. **117**, 228 (1986).
[17] A. Yiannopoulou, K. Urbanski, S. Antonova, A. M. Lyyra, Li Li, T. An, B. Ji, and W. C. Stwalley, J. Mol. Spectrosc. **172**, 567 (1995).
[18] A. Yiannopoulou, K. Urbanski, S. Antonova, A. M. Lyyra, Li Li, T. An, T.-J. Whang, B. Ji, X. Wang, W. C. Stwalley, T. Leininger, and G.-H. Jeug, J. Chem. Phys. **103**, 5898 (1995).
[19] R. S. Freund, T. A. Miller, R. Jost, and M. Lombardi, J. Chem. Phys. **68**, 1683 (1978).
[20] T. A. Miller, R. S. Freund, and B. R. Zegarski, J. Chem. Phys. **64**, 1842 (1976).
[21] L. Sibbach, P. Burns, and J. Huennekens (unpublished).
[22] H. Katô, M. Sakano, N. Yoshie, M. Baba, and K. Ishikawa, J. Chem. Phys. **93**, 2228 (1990).
[23] M. Baba, K. Nishizawa, N. Yoshie, K. Ishikawa, and H. Katô, J. Chem. Phys. **96**, 955 (1992).
[24] P. Kowalczyk, B. Krüger, and F. Engelke, Chem. Phys. Lett. **147**, 301 (1988).
[25] P. Kowalczyk, J. Chem. Phys. **91**, 2779 (1989).
[26] K. Ishikawa, T. Kumauchi, M. Baba, and H. Katô, J. Chem. Phys. **96**, 6423 (1992).
[27] Li Li, S. F. Rice, and R. W. Field, J. Chem. Phys. **82**, 1178 (1985).
[28] A. Färbert and W. Demtröder, Chem. Phys. Lett. **264**, 225 (1997).
[29] K. Ishikawa, J. Chem. Phys. **98**, 1916 (1993).
[30] K. Ishikawa, N. Mukai, and M. Tanimura, J. Chem. Phys. **101**, 876 (1994).
[31] Z. W. Fu, E. A. Hessels, and S. R. Lundeen, Phys. Rev. A **46**, R5313 (1992).

Downloaded 25 Aug 2002 to 128.180.23.36. Redistribution subject to AIP license or copyright, see http://ojps.aip.org/jcpo/jcpcr.jsp